



# Application of graphene oxide/titanium dioxide nanoparticle on the rheological, filtration and shale swelling characteristics in water-based mud system: experimental and full factorial design study

Shaine Mohammadali Lalji<sup>1</sup> · Javed Haneef<sup>1</sup> · Saud Hashmi<sup>2</sup>

Received: 26 September 2023 / Accepted: 8 April 2024 / Published online: 29 April 2024  
© The Author(s), under exclusive licence to the Institute of Chemistry, Slovak Academy of Sciences 2024

## Abstract

Wellbore instability because of poor rheological properties, high fluid loss volume and shale swelling is the leading challenge faced by the petroleum sector. Therefore, the success of any drilling activity is fundamentally governed by the characteristics of the drilling mud. The main scope of this study is to observe an increase in the performance of water-based mud (WBM) after the addition of synthesized GO/TiO<sub>2</sub> nanoparticles. In the first part, properties of WBM are analyzed after the addition of GO/TiO<sub>2</sub> and anatase-TiO<sub>2</sub> nanoparticles. Each particles as a separate entity is added in different three concentrations (0.75, 1.5, 2.25 g) in the WBM. In the second part, the influence of salt, polymer and synthesized nanoparticles on inhibiting the shale swelling is observed. For the first part, the results reveal that the rheological properties of all the six samples are in the API recommended window. However, plastic viscosity, yield point, gel strength (10 s/10 min), and transport index of the base mud substantially improves with the addition of GO/TiO<sub>2</sub> nanoparticles than anatase-TiO<sub>2</sub> nanoparticles. Furthermore, the GO supports TiO<sub>2</sub> through oxygen-bearing functional groups, which eventually improves the adsorptivity of GO/TiO<sub>2</sub> particles in the micro and nanopores and decreases the filtrate loss volume. Thin and compacted mud cake with lower permeability is obtain from GO/TiO<sub>2</sub> nanoparticles. For the second part, full factorial design of experiment technique is implemented on the shale swelling behavior. The result of this segment indicates that GO/TiO<sub>2</sub> nanoparticles are the most influential factor in reducing the shale swelling behavior. The shale surface becomes hydrophobic after its interaction with the GO/TiO<sub>2</sub> nanoparticles. Moreover, these particles are responsible for developing strong interparticle hydrogen bonds between themselves, which prevents the fluid migration into the shale pellets. On the other hand, the impact of KCl and PAC on the shale swelling is relatively small. The polymer PAC is dehydrated in the presence of monovalent cations, which impacts their performance in minimizing the shale swelling.

**Keywords** Titanium dioxide · GO/TiO<sub>2</sub> · Rheological properties · Filtration properties · Full factorial design · PAC

## List of symbols

TiO<sub>2</sub> Titanium dioxide  
WBM Water-based mud

OBM Oil-based mud  
KCl Potassium chloride  
PAC Polyanionic cellulose  
FFD Full factorial design  
PV Plastic viscosity  
YP Yield point  
GS Gel strength  
AV Apparent viscosity  
LPLT Low pressure low temperature  
mD Milli-darcy

✉ Saud Hashmi  
saudhashmi@neduet.edu.pk

Shaine Mohammadali Lalji  
shaine@neduet.edu.pk

Javed Haneef  
javedh@neduet.edu.pk

<sup>1</sup> Department of Petroleum Engineering, NED University of Engineering and Technology, Karachi, Pakistan

<sup>2</sup> Department of Chemical Engineering, NED University of Engineering and Technology, Karachi, Pakistan

## Introduction

Drilling is a fundamental and costly process in the oil and gas sector. The key element of any drilling activity is the preparation of the drilling mud, which is responsible for performing many functions over the course of the entire drilling activity (Wajheuddin and Hossian 2018). The main characteristics of drilling mud is to remove and lift the drill cutting from the bottom of the borehole up to the surface, maintain the integrity of the wellbore, cool the drill bit and the drill pipes, and maintain adequate hydrostatic pressure inside the wellbore (Wajheuddin and Hossian 2018; Lalji et al. 2023a). Among all the mud systems, water-based mud (WBM) is the most frequently used type of mud used in drilling operations. The WBM system is environmentally friendly, less costly, and is easy to formulate. However, differential sticking, shale instability, loss of circulation, caving and washouts are some common problems associated with WBM (Wajheuddin and Hossian 2018; Lalji and Ali 2023; Lalji et al. 2023b). Therefore, numerous scholars are continuously working on improving the characteristics of WBM for the purpose of reducing the problems associated with this system.

Initially, the performance of WBM was improved with the addition of salt, most commonly known as potassium chloride (KCl). This additive was effective in maintaining the rheological behavior of WBM in the desired range, and also increased the shale stability (Mohamed Khodja et al. 2010). However, at higher concentration, KCl dephase the mud into two separate entities (Chang and Leong 2014). Consequently, the application of polymers in enhancing properties of drilling fluid gains substantial importance in the oil and gas sector. Various polymeric materials with their unique characteristics were used by numerous researchers in the WBM system to improve its characteristics. These polymeric materials include partially hydrolyzed polyacrylamide (PHPA), poly anionic cellulose (PAC), hydroxyethyl cellulose (HEC), and carboxymethyl cellulose (CEC) (Jefferis et al. 2015). However, their use is limited to a certain extent because of their expensive nature, incapability with anionic additives, and inability to work at elevated temperature conditions (Aftab et al. 2017). Therefore, the petroleum industry is exploring new alternatives, which have all the desired properties to enhance the performance of WBM and can also challenge the shortcoming associated with the polymers. Consequently, the use of nanomaterials in drilling fluid gains significant importance. This technology opens new and diverse doors in the field of drilling engineering especially in the area of drilling mud.

Several nanoparticles have been studied by numerous scholars and their positive impact on the properties

of drilling fluid are documented in the literature (Hoelscher et al. 2012; Ravi Kumar 2019; Mortadha Alsaba et al. 2019). The most commonly used nanoparticles are silica (Boul et al. 2016), graphene oxide (Aramendiz and Imqam 2020a), iron oxide (Alvi et al. 2020), copper oxide (Ponmani et al. 2016), zinc oxide (Ponmani et al. 2016). However, limited attention is given to titanium dioxide ( $\text{TiO}_2$ ) nanoparticles as a drilling mud additive.

$\text{TiO}_2$  nanoparticles play a prominent role in the areas of photo-catalysis, paints, cosmetics and many more (Reghunath et al. 2021). This metal oxide nanoparticle is capable of providing high chemical stability and substantial electrochemical properties (Reghunath et al. 2021). In addition, the non-toxic nature and commercially viable nature are some of other possible causes for its effectiveness. All these properties associated with  $\text{TiO}_2$  nanoparticles are mainly due to its crystal structure, large surface area, and noble metallic loading (Reghunath et al. 2021). In general, this nanoparticle exists in four major crystal systems, which includes anatase, rutile, brookite and  $\text{TiO}_2$ -B (Reghunath et al. 2021). At nanoscale dimensions, anatase and brookite are the most stable crystal forms of  $\text{TiO}_2$  nanoparticles (Altomare et al. 2015). However, the large band gap in the anatase crystal system substantially affects its performance. To improve the characteristics of  $\text{TiO}_2$  nanoparticles, various support systems are provided. The most effective support system is provided with the help of the carbonaceous materials. Among all the carbonaceous material, graphene oxide gains significant attention due to its unique two-dimensional geometry, high conductivity and large surface area (Mahima Sharma 2018).

Graphene-based nanostructures have numerous applications due to their unique characteristics. These nanomaterials are currently used in energy-based zones of modern technology for the purpose of energy storage in the form of fuel cell, lithium batteries, super-capacitors, and photocatalysts (Yusaf et al. 2022). Moreover, due to their high surface area, easy surface functionalization, and selective properties, these nanostructures are also used for gene and drug delivery in the field of medicine (Liu et al. 2014). Additionally, the recent advancement in graphene-based nanomaterials offer novel and advanced methods to deal with malignancy (You et al. 2015). Besides this, these structures are also now part of our personal computers, mobile phones and tablets, making them advanced and fast-processing (Yusaf et al. 2022). Furthermore, graphene nanostructures are also used in the food packing industry. These advanced nanomaterials contain antimicrobial mechanisms, which inhibit microbial growth and affect the physical metabolism developments (Romanchuk et al. 2013). Despite all these recent developments, the use of graphene-based nanostructures are limited in the field of drilling fluids.

In the current work, the performance of TiO<sub>2</sub> and GO/TiO<sub>2</sub> nanoparticles in drilling fluid was investigated. A series of rheological, filtration, and shale swelling tests were conducted and were examined. Based on the experimental results, the efficacy of GO/TiO<sub>2</sub> nanoparticles in drilling fluid was observed. Moreover, the performance of GO/TiO<sub>2</sub> nanoparticles in mitigating the shale swelling was also evaluated using 2<sup>n</sup> factorial analysis. In this investigation, the impact of KCl, PAC and GO/TiO<sub>2</sub> nanoparticles was examined and the most influential additive for the shale swelling behavior was obtained. For the first time, this type of comparison between salt, polymer and nanoparticle was analyzed using the 2<sup>n</sup> factorial approach.

### Previous studies on GO and TiO<sub>2</sub> particles in drilling mud

Several applications of GO and TiO<sub>2</sub> nanoparticles as drilling fluid additives have been reported in the literature. These particles are commonly added in drilling fluid to enhance the characteristics of the mud system. Some of the most recent

work conducted by numerous scholars on these particles along with their findings are presented in Table 1.

## Material and methods

### Materials

The materials required for the synthesis of nanoparticles and for the formulation drilling mud were acquired from various sources. Table 2 shows the complete information related to the particles source.

### Synthesis of GO/TiO<sub>2</sub> nanoparticle

The GO/TiO<sub>2</sub> nanoparticle was synthesized using the hydrothermal thermal technique. For the synthesis of GO/TiO<sub>2</sub> nanoparticle, GO was provided purchased from Xi'an Lyphar Biotech Co. Ltd. The complete characterization detail can be found out in our previous study (Lalji et al. 2023c). The oxygenated functional groups were also provided by the vendor. Initially, the graphene oxide was mixed

**Table 1** Selected work on the GO and TiO<sub>2</sub> nanoparticles as drilling fluid additives

Particle	Type of drilling fluid	Concentration of particles	Result	References
Novel tailor-made TiO <sub>2</sub> nanoparticles-bentonite (TNBT) nanocomposites	WBM	0 to 1 g	Improvement in rheological properties	Adnan Aftab et al. (2020)
SiO <sub>2</sub> and TiO <sub>2</sub>	WBM	0.01–0.5 wt.%	Changes in rheological properties. TiO <sub>2</sub> reduces yield point of the mud. Both particles help in reducing the fluid loss	Bayat et al. (2021)
PAAN and PAAN-G (Acrylamide polymer/graphene oxide composite)	WBM	1 wt.%	GO thermal stability greatly improved after compositing with polymer. Loss of filtrate volume was also minimized	Jingyuan Ma (2021)
GO	WBM	0.01–0.5 wt.%	Drilling fluid with nanoparticles shows less erosion and cracks, better rheological properties, and lower shale swelling	Lalji et al. (2022)
GO	WBM	0.2, 0.4, 0.6, 0.8%	GO showed improved performances on reducing the swelling rate	Kai Wang 2020)
SiO <sub>2</sub> , TiO <sub>2</sub> , Al <sub>2</sub> O <sub>3</sub>	WBM	0-2wt.%	Improvement in rheological properties, decrease in filtration loss, maximum decrease in friction force	Minakov et al. (2018)
GO and GO-Zn composite	WBM	0.1, 0.3	Increase in rheological properties, decrease the filtrate loss,	Ali Ghayedi (2020)
Silica and Graphene Oxide NPs	KCL/PHPA WBM	0.25–0.5wt%	Improvement in overall properties of a WBM and its long-term stability under aging condition	Aramendiz and Imqam (2020b)

**Table 2** Materials used for the synthesis of nanoparticles and in the preparation of WBM

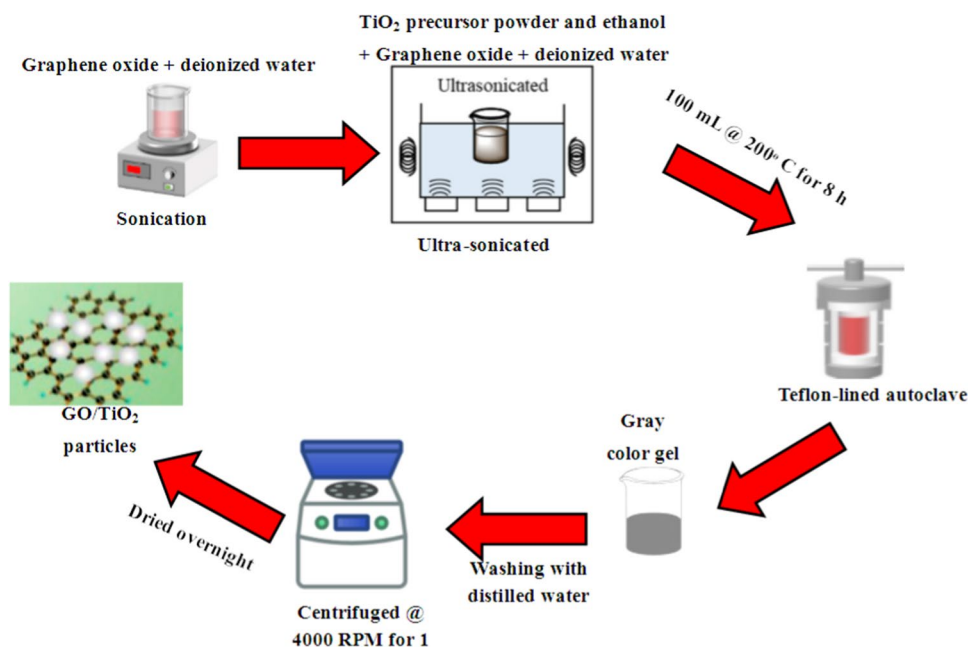
Component	Use	Source
Graphene oxide	Synthesis of GO/TiO <sub>2</sub> nanoparticle	Xi'an Lyphar Biotech Co. Ltd
Deionized water	Synthesis of GO/TiO <sub>2</sub> nanoparticle	Local vendor
TiO <sub>2</sub> precursor (Titanium (VI) isopropoxide)	Synthesis of GO/TiO <sub>2</sub> nanoparticle	Sigma-Aldrich
Ethanol	Synthesis of GO/TiO <sub>2</sub> nanoparticle	Local vendor
Teflon-lined autoclave	Synthesis of GO/TiO <sub>2</sub> nanoparticle	Local vendor
Sodium hydroxide	Stability of solvent	Sigma-Aldrich
Centrifuge	Mixing at higher RPMs	Local vendor
Tap Water	Continuous phase in drilling mud	Tap water
Sodium carbonate (Na <sub>2</sub> CO <sub>3</sub> )	Treatment of water	Sigma-Aldrich
Potassium chloride (KCl)	Shale Stabilizer	Sigma-Aldrich
Polyanionic cellulose (PAC)	Shale Stabilizer and filtration reduction	Sigma-Aldrich
Barite	Weighting agent	Sigma-Aldrich

with the deionized water and then exfoliated through sonication for one hour. Next, a paste prepared from the TiO<sub>2</sub> precursor powder and ethanol was added drop wise to the GO solution and mixed vigorously. The mixture was ultrasonicated for one hour before transferring it into a Teflon-lined autoclave. Moreover, before the transferring process, a small concentration of sodium hydroxide is added to the mixture for the purpose of maintaining the pH. Next, 100 mL of prepared solution was transferred into a Teflon-lined autoclave and heated at 200 °C for 8 h. A gray gel colored sample was collected, which was then washed with distilled water several times to remove any impurities. The final product was centrifuged at 4000 RPM for one hour and then was dried overnight to obtain GO/TiO<sub>2</sub> nanoparticles.

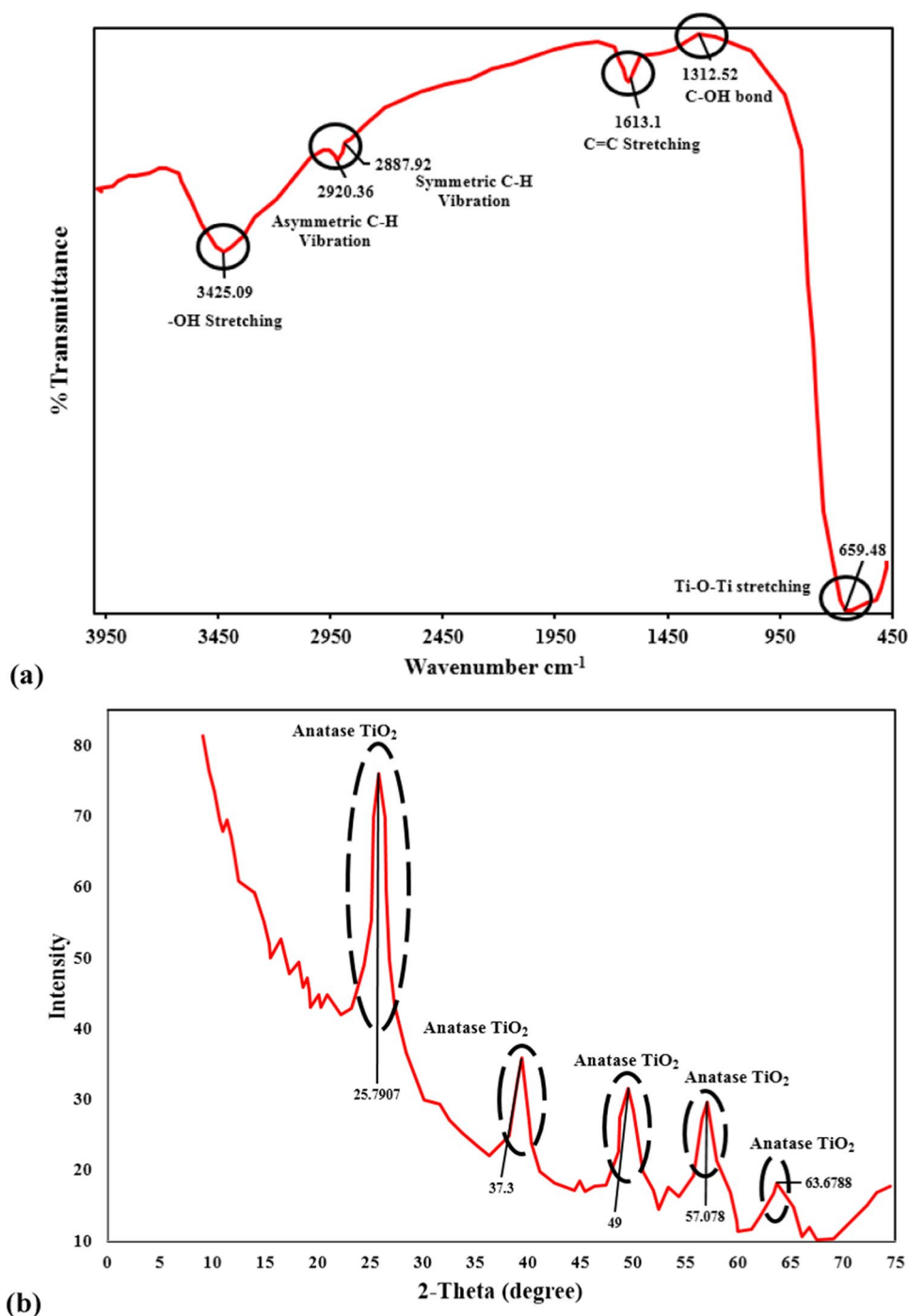
Figure 1 displayed the schematic for the synthesis of GO/TiO<sub>2</sub> nanoparticles.

### Characterization of Particles

Figure 2a shows the Fourier transform infrared analysis of a GO/TiO<sub>2</sub> nanoparticle. The strong characterization peak obtained at 3425.09 cm<sup>-1</sup> corresponds to the elongation of O–H bond in graphene oxide and its composites with titanium dioxide (Nethravathi and Rajamathi 2008). The peak at 2920.36 cm<sup>-1</sup> corresponds to the asymmetric movements of the C–H. On the other hand, the small peak at 2887.92 cm<sup>-1</sup> indicates symmetric movements of C–H bond. The presence of characterization

**Fig. 1** Schematic for the synthesis of GO/TiO<sub>2</sub> nanoparticles

**Fig. 2** Characterization GO/TiO<sub>2</sub> nanoparticle used in this study **a** FTIR spectrum, **b** XRD analysis



peak at  $1613.1\text{ cm}^{-1}$  indicates the skeletal vibrations of non-oxidized graphitic domains, which is mainly due to the stretching vibrations of C=C (Shen et al. 2011). The peak at  $1312.52\text{ cm}^{-1}$  indicates the C–OH stretching vibration of the alkoxy functional group along with Ti–O modes. Finally, the broad peak obtained between  $500\text{--}1000\text{ cm}^{-1}$  specifies the Ti–O–Ti stretching present in the nanoparticle (Yu et al. 2006). This characterization peak is mainly due to the chemical relations between the

functional groups associated with graphene oxide and the surface hydroxyl groups present in TiO<sub>2</sub> (Nguyen-Phan, et al. 2011). Figure 2b shows the XRD analysis of the GO/TiO<sub>2</sub> nanoparticle. The 2-theta peaks at  $25.1$ ,  $37.3$ ,  $49$ ,  $57.1$ ,  $63.68^\circ$  show the presence of anatase-TiO<sub>2</sub>. The peak of graphene oxide at  $24.6^\circ$  was curtailed by anatase-TiO<sub>2</sub> peak at  $25.1^\circ$ . At lower concentration, the graphene oxide peak is usually overpowered by anatase-TiO<sub>2</sub>. The crystalline size of the nanoparticles was measured using

Debye–Scherrer equation. During the study, the average crystalline size of the nanoparticles was 12.45 nm.

### Formulation of water-base mud

The water-based mud was prepared using the solution method also known as the direct mixing method. This technique is most suitable for the formulation of a water-based mud system. Table 3 displays the composition of each sample prepared in this study. According to API recommended protocol, one barrel equivalent to 350 cc of mud was prepared using Hamilton beach stirrer. The mixing of the mud was continued until a stable mud sample with proper dispersed NPs was achieved. Both the tested particles were added in the base mud sample in various concentrations of 0.75, 1.5 and 2.25 g. The 2.25 g of nanoparticle corresponds to 0.65 wt. %. According to Parizad et al. in (2019), increasing the concentration of TiO<sub>2</sub> particles beyond 0.75% is not economical and effective for the mud system (Amirhossein Parizad et al. 2019). Hence, during this study, experiments are designed on the bases of Parizad et al. threshold limit. In this way, a substantial quantity of resources and time were preserved.

The main aim was to investigate the performance enhancement in TiO<sub>2</sub> NPs WBM after it has been supported by a carbonaceous material. Figure 3 shows the complete experimental procedure followed the course of study.

### Mud weight

Density of drilling fluid is a critical factor during any drilling operation. This parameter is responsible for maintaining the desired hydrostatic pressure within the borehole, and at the same time prevents the unwanted flow within the wellbore (Ali et al. 2022). In the laboratory, this property is measured using an apparatus known as mud balance, which is an effective way of measuring the mud density (Ali et al. 2022). Drilling fluids will lower mud weight are usually are responsible for creating

problem like caving and washouts. On the other hand, higher density muds are accountable for causing formation damage and loss circulation problems (Rafieefar 2021). During this study, the density of the base mud was 10 ppg, which remained unaffected by the addition of nanoparticles. In addition, no significant influence on the mud weight was recorded due to temperature (Ali et al. 2022).

### Rheological characteristics

The rheological properties were investigated using the FANN 35 rheometer (MODEL-286). Rheological characteristics such as plastic viscosity (PV), yield point (YP), apparent viscosity (AV), gel strength (GS) and YP/PV (Transport Index) ratio were all measured at a room temperature of 30 °C. During the study, the shear rate was maintained in between the ranges of 600–100 s<sup>-1</sup>. The API recommended practices were thoroughly followed during the measurement of rheological properties (Institute 2017). Equations 1–3 were used to compute the rheological behavior of each fluid system. The parameters  $\theta_{600}$  and  $\theta_{300}$  are dial reading obtained from FANN viscometer. For the GS 10 s testing, the sample was rotated at the 600 RPM, followed by a static period of 10 s. After 10 s, the sample was rotated at 3 RPM and the maximum change in the rheometer dial was recorded (Ali et al. 2022). Similar procedure was followed for GS 10 min; however, this time around the static period was observed for 10 min.

$$\text{Plastic viscosity (cP)} = \theta_{600} - \theta_{300} \quad (1)$$

$$\text{Yield point} \left( \frac{\text{lb}}{100\text{ft}^2} \right) = \theta_{300} - \text{plastic viscosity} \quad (2)$$

$$\text{Apparent viscosity (cP)} = \frac{\theta_{600}}{2} \quad (3)$$

**Table 3** Composition of all the studied mud sample in this work

Component	Base Mud	TiO <sub>2</sub> -WBM (S <sub>1</sub> )	TiO <sub>2</sub> -WBM (S <sub>2</sub> )	TiO <sub>2</sub> -WBM (S <sub>3</sub> )	GO/TiO <sub>2</sub> -WBM (S <sub>4</sub> )	GO/TiO <sub>2</sub> -WBM (S <sub>5</sub> )	GO/TiO <sub>2</sub> -WBM (S <sub>6</sub> )
Distilled Water (mL)	320	320	320	320	320	320	320
KCl (g)	18	18	18	18	18	18	18
Na <sub>2</sub> CO <sub>3</sub> (g)	0.25	0.25	0.25	0.25	0.25	0.25	0.25
PAC (g)	4.25	4.25	4.25	4.25	4.25	4.25	4.25
Barite (g)	82	82	82	82	82	82	82
Anatase-TiO <sub>2</sub> (g)	X	0.75	1.50	2.25	X	X	X
GO/TiO <sub>2</sub> (g)	X	X	X	X	0.75	1.50	2.25

S<sub>n</sub> = sample number



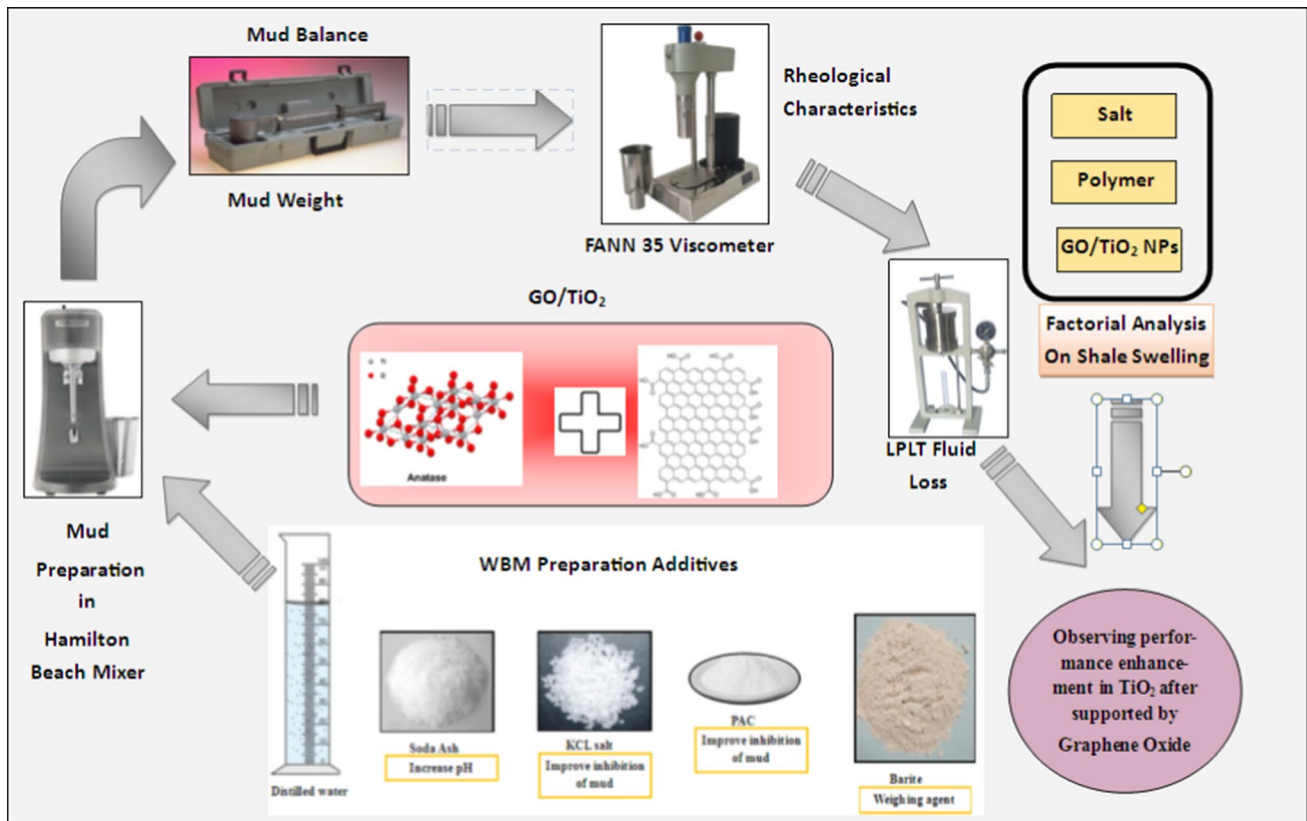


Fig. 3 Experimental flowchart followed during this study

### API filter press (low pressure low temperature)

The LPLT API Filter press was performed on each of the samples. All the filter press testing was conducted at an ambient condition of 30 °C and a differential pressure of 100 psi. The removal of mud filtrate from the mud system was recorded on every five minute interval till standard 30 min. Moreover, the filter cakes that were collected at the end of experimentation were also investigated for thickness, permeability and texture. During API filter press testing, the API protocols were meticulously followed. The uncertainty associated with the experimentation was kept within the acceptable boundary of 2%.

### Liner dynamic swell-meter (LDSM)

During LDSM testing, shale cuttings were first dried in an oven for about 150 °C to remove any moisture content. Next, the dried samples were crushed and converted into the fine powder form using Mortar Grinder. The prepared powder was then passed through the sieve shaker, and the fine powder collected on the 0.212 mm sieve was used for further analysis. The 15 g of fine powder was then placed in a hydraulic compactor for about 30 min at a pressure of

6000 psi to form cylindrical shale pellets. These pellets were then placed into the LDSM where it interacts with the tested mud sample for approximately 24 h to monitor the changes in shale behavior. Once the equilibrium state was achieved in the LDSM testing, the swelling experiment was stopped, and the final swelling percentage was recorded. In general, a lower shale swelling percentage indicates toward the higher efficacy of the mud.

### Full factorial design (FFD) of experiment

A comparison study was also conducted to evaluate the efficiency of GO/TiO<sub>2</sub> nanoparticles over a salt and a polymeric material. During this investigation, the shale swelling was tested and the most influential additive out of GO/TiO<sub>2</sub> nanoparticles, KCl and PAC was determined. During this study, FFD was implemented and the impact of additives (KCl, PAC and GO/TiO<sub>2</sub>) on shale swelling was investigated. Each factor is divided into 2 levels and based on the mathematical expression 2<sup>n</sup> shale swelling tests were conducted. In this study, ‘8’ runs were evaluated. This tool provides an insight information of the system, thus making it an effective tool to investigate the performance of each variable (Aleksandar Jankovic and Goia 2021).

## Result and discussion

### Effect of particles on flow curve

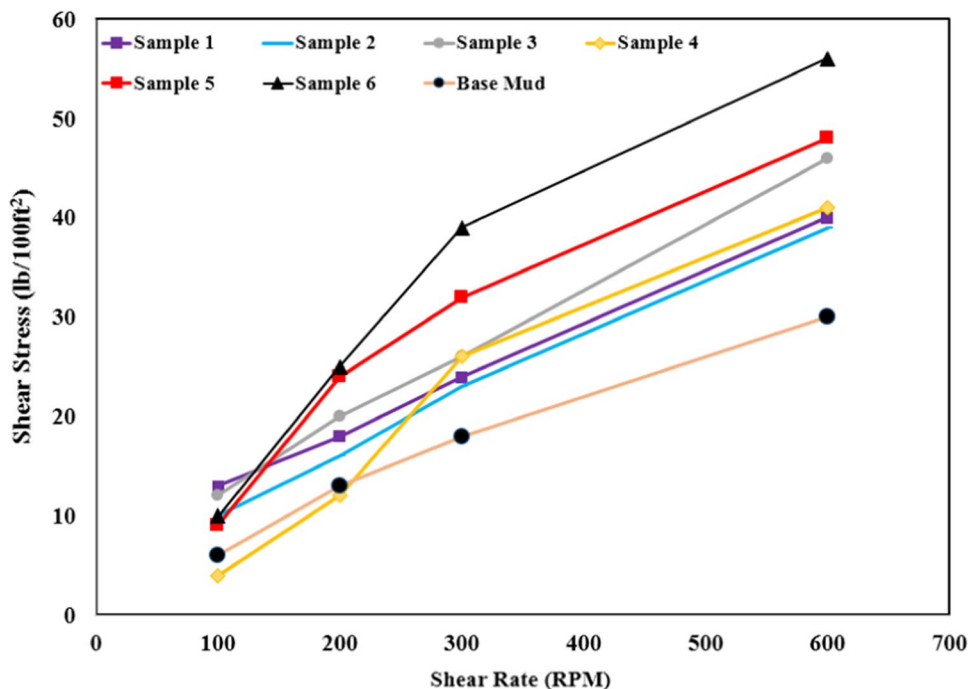
Figure 4 depicts the rheogram showing the relationship between shear stress and shear rate of all the studied samples. At constant shear rate, the shear stress rises with an increase in particle concentration. Based on the rheogram, each non-Newtonian fluid demonstrates pseudo plastic or shear thinning characteristics. An upsurge in shear rate will cause a reduction in viscosity of the sample. This behavior is essential, as at static condition, high viscosity is required for the suspension of the drilled cutting and during dynamic condition, lower viscosity is vital, which assists in the removal of the drilled cutting on to the rig site (Ahmed et al. 2020). The lowest shear stress was observed in the base mud sample, which improves with the addition of NPs. The highest shear stresses were recorded in  $S_5$  and  $S_6$ . Both of these samples contains the highest concentration of GO/TiO<sub>2</sub> NPs. Shear stress in presence of 2.25 g of GO/TiO<sub>2</sub> NPs was double that of the base mud.

In these samples, the sheets of GO/TiO<sub>2</sub> were well dispersed throughout the water suspension. Subsequently, a hydrogen bond between GO/TiO<sub>2</sub> NPs and PAC can be developed, which becomes substantially stronger as GO/TiO<sub>2</sub> NPs concentration increases. This results in an increase in flow resistance and ultimately intensifies the viscosity and the shear stress.

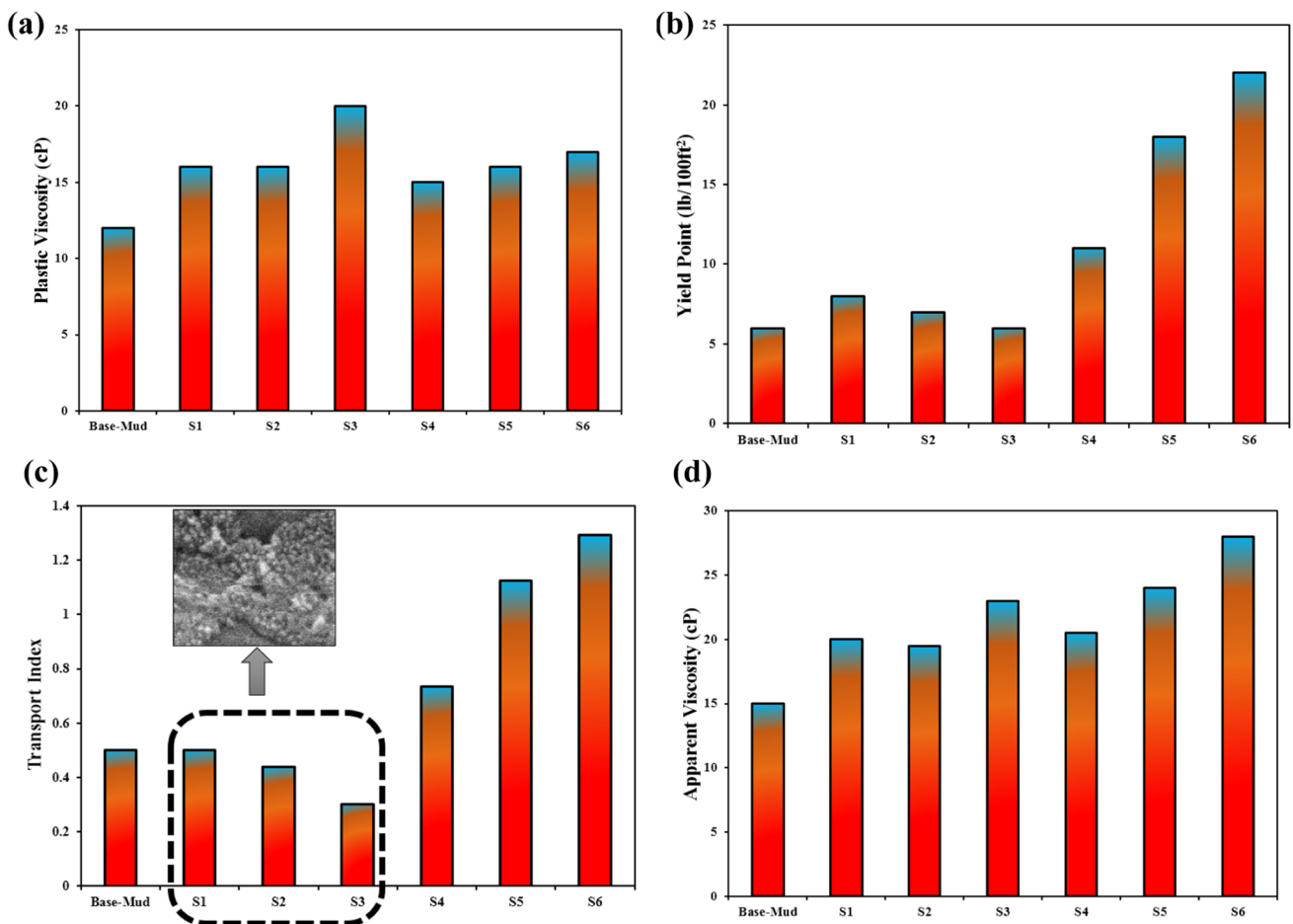
### Effect of particles on Rheological properties

Figure 5a–d shows the rheological properties of all the six studied samples. The parameters were recorded using the FANN 35 rheometer and were calculated using Eqs. (1–3). Figure 5a represents the plastic viscosity (PV) of each sample. Plastic viscosity is defined as the friction force arises between the solid particles and in between the individual fluid layer of the system (Elkatatny 2019). In general, fluids demonstrated high PV are difficult to pump, while lower PV exhibit incapability in the transportation of the drilled cutting (Bayat et al. 2018a). Hence, maintaining an optimum PV is crucial during any drilling activity. According to the American Petroleum Institute (API), the recommended value for PV for any drilling fluid should be in range of 8–35 cP (Biwott 2019). During the experimentation, PV of all the studied samples fall within the API suggested range as depicted in Fig. 5a. Moreover, an increase in PV was recorded when the quantity of the nanoparticles increases in the drilling mud. The base mud with composition shown in Table 3 shows the PV of 12 cP. With the introduction of the nanoparticles, PV increases and goes above the PV of the base mud. This result is in good agreement with Smoluchowski's modification of Einstein equation (Aftab et al. 2016), which explains the relationship between the particle size and PV. The maximum PV (20 cP) was recorded in Sample 3 consists of 2.25 g of TiO<sub>2</sub>. Similar characteristics were also demonstrated by GO/TiO<sub>2</sub> NPs. The modified TiO<sub>2</sub> NPs also displayed a higher PV than the base mud sample. Different scholars

**Fig. 4** Rheogram of studied mud samples







**Fig. 5** Rheological parameters of each studied sample. **a** Plastic viscosity, **b** yield point, **c** YP/PV ratio, **d** apparent viscosity

had conducted research on GO and TiO<sub>2</sub> NPs, but there is no case reported that investigated the combined impact of both these additives. Bayat et al. (2018a) conducted a study on TiO<sub>2</sub> NPs. According to the study, the maximum PV attained after using TiO<sub>2</sub> NPs was 10 cP at 0.01 wt. % that reached to 9 cP at the concentration of 1 wt. % (Bayat et al. 2018a). On the other hand, Rafieefar et al. (2021) reported the PV for the GO. According to the study, the maximum PV attained was 11 cP at 0.15 wt. % (Rafieefar 2021). A significant improvement in PV was observed when TiO<sub>2</sub> NPs was supported with GO. By adding 0.75 g GO/TiO<sub>2</sub> NPs to the base mud, the PV attained was 15 cP. With increasing the quantity of GO/TiO<sub>2</sub> NPs up to 2.25 g, the PV was 17 cP. The enhancement of PV is mainly due to the dispersion of nanoparticles between the fluid layers, which eventually increases the fluid internal resistance and increases the plastic viscosity (Sundar et al. 2013). This investigation clearly shows the GO/TiO<sub>2</sub> NPs is extremely effective than TiO<sub>2</sub> and GO separately in maintain the PV, which eventually impacts the hydrostatic pressure of the mud in the wellbore and assist in safe drilling activity.

Figure 5b represents the yield point (YP) of all the studied mud samples. The YP represents the electrochemical forces, which creates friction during the fluid flow (Bayat et al. 2018a). According to API recommended practices, YP should not go below 5 lb/100 ft<sup>2</sup> and should not exceed 3xPV (Biwott 2019). The results showed that all the studied samples YP fall under the prescribed range of API. The YP for the TiO<sub>2</sub> particle remained closer to the base mud. According to Parizad et al. in 2019, increasing the concentration of TiO<sub>2</sub> particles beyond 0.75% is not economical and effective for the mud system (Amirhossein Parizad et al. 2019). This statement was in good agreement with the current work, as when TiO<sub>2</sub> particle concentration starts to increase in the mud the YP decreases. Beg (2020) studied TiO<sub>2</sub> particles as a separate entity (Mukarram Beg 2020). When this particle was added to the base mud, YP of 12 lb/100 ft<sup>2</sup> was recorded at 25 °C. Similarly, Lalji et al. (2022) studied the influence of GO on salt-polymer mud and observed a 17 lb/100 ft<sup>2</sup> at 0.4 wt. % (Lalji et al. 2022). However, when TiO<sub>2</sub> particles was coated with GO, a substantial increase in YP was recorded. As the dimension of

particles reduces an increase in YP was recorded (Rafieefar 2021). The smaller dimension particles improve the attractive forces between the positive and negative charges, which eventually increases the YP (Aftab et al. 2016). The GO/TiO<sub>2</sub> particle declines the agglomeration among the drilling fluid particles and improves the YP, which eventually helps in the transportation of drilled cuttings to the ground surface better than GO and TiO<sub>2</sub> as separate entities.

Furthermore, the cutting lifting efficiency of each studied sample was also examined using the YP/PV ratio, also commonly known as Transport Index (TI). According to APT 13A specification, this ratio should be in range of 0.7–1.5 for any drilling fluid (Elkatatny 2019). The magnitude of this ratio specifies the effectiveness of a drilling fluid in minimizing the cutting volume in the annulus, which ultimately avoids any differential sticking problems (Elkatatny 2019). Based on the findings, it can be witnessed from Fig. 5c that the inclusion of the GO/TiO<sub>2</sub> particle improves the YP and PV of the drilling mud and improves the ratio according to APT 13A specification. For the base mud and TiO<sub>2</sub> particles mud systems, this ratio falls well below the APT 13A specification. The lower magnitude of YP was the main reason behind its failure. In addition, at higher concentration, TiO<sub>2</sub> particles forms clusters as shown by the SEM image in Fig. 5c. This further decreases the performance of the TiO<sub>2</sub> particles mud, as the performance of nanoparticles was suppressed in the WBM.

Figure 5d shows the apparent viscosity (AV) of each of the six studied particles. According to API standards, a fluid should demonstrate at least 12–cP of AV (Dankwa et al. 2018). Beg (2020) studied the AV of TiO<sub>2</sub> NPs. According to their finding, the base mud with TiO<sub>2</sub> NPs demonstrated AV of 15 cP at 25 °C (Mukarram Beg 2020). Moreover, according to Lalji et al. (2021), when GO was used in WBM, the AV of the base mud remained fairly constant at 17 cP, and remained independent of GO concentration (Lalji et al. 2023c). In the current work, it can be observed that the AV of base mud was 15 cP, which substantially improves as the quantity of the nanoparticles increases. With the addition of NPs, the fluid becomes more viscous, which eventually elevates the AV. Moreover, the maximum AV was recorded in mud that contains the maximum concentration of GO/TiO<sub>2</sub> particles. This clearly shows that when the TiO<sub>2</sub> NPs was supported with GO, the thixotropic characteristics of drilling mud increases, which eventually increases the fluid performance in the wellbore.

### Influence of particles on Gel strength (GS)

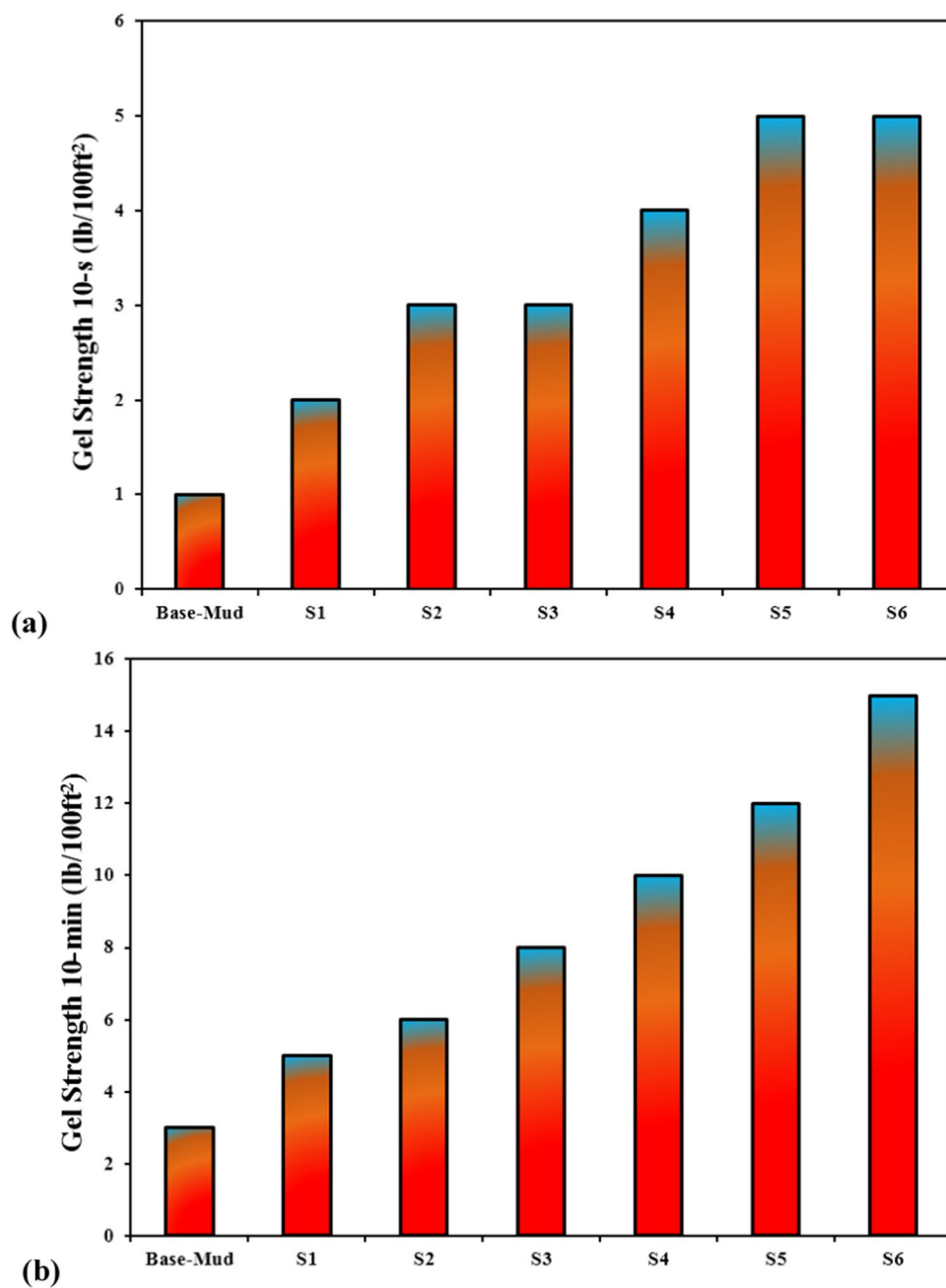
Figure 6a, b depicts the GS recorded at 10 s and 10 min intervals for all the studied mud samples. The GS of any mud provides information on the ability of the drilling fluid to suspend the drilled cuttings under static conditions

(Lalji et al. 2023c). According to API recommended practices, a drilling fluid should exhibit GS 10 s in range of 2 – 5 lb/100 ft<sup>2</sup> (Biwott 2019). Fluids that display lower GS as prescribed by API will suffer cutting transportation problems. On the other hand, higher GS fluids demand high pumping rates, nevertheless, sometimes it is effective to have higher GS in order to mitigate different drilling related problems. Beg (2020) studied the 10 s GS and 10 min GS of TiO<sub>2</sub> NPs. According to their investigation, the base mud with TiO<sub>2</sub> NPs demonstrated 7lb/100 ft<sup>2</sup> and 10 lb/100 ft<sup>2</sup> of 10 s GS and 10 min GS, respectively (Beg 2020). The 10 s GS in Beg (2020) was above the API recommended practices, which clearly indicates a higher pump pressure requirement for this mud system. On the other hand, the study conducted by Lalji et al. (2021) shows that when GO was used in the base mud, the 10 s GS rose from 6 lb/100 ft<sup>2</sup> at 0.1 wt. % to 8 lb/100 ft<sup>2</sup> at 0.5 wt. %, going beyond the API protocols. Additionally, 10 min GS remained constant at 8 lb/100 ft<sup>2</sup> (Lalji et al. 2023c). During the experimental investigation, the 10 s and 10 min GS of the base mud were 1 lb/100 ft<sup>2</sup>, which were lower than the API prescribed range. However, with the addition of particles it improves and goes in the desired range. Moreover, GO/TiO<sub>2</sub> particles showed more efficacy by increasing GS higher than TiO<sub>2</sub> particles as shown in Fig. 6a. However, both particles show flat rheology, which indicates no substantial changes in GS with time (Elkatatny 2019). Figure 6b shows the GS measured at a 10 min interval. According to API recommended practices, a drilling fluid should exhibit GS 10 min in range of 2 – 35 lb/100 ft<sup>2</sup> (Biwott 2019). 10 min GS was substantially improved with the addition of TiO<sub>2</sub> and synthesized GO/TiO<sub>2</sub> particles. However, when the TiO<sub>2</sub> particles are supported with GO, the efficacy of the particles increases, which improves the gelation and cutting suspension characteristics of the base mud. Moreover, all the six samples were capable enough to make the drilled cuttings suspended when experiencing static conditions.

### Effect of particle on filtrate volume loss

The amount of water separated from the mud system is measured using API low pressure and low temperature filter press test. Drilling mud that demonstrates high fluid loss volume is undesirable as it gives rise to complications such as formation damage and wellbore instability (Deng et al. 2015). According to Beg (2020) study, the base mud with TiO<sub>2</sub> NPs showed 30.2 mL of fluid loss before the hot rolling test (Mukarram Beg 2020). Moreover, a filtrate volume of 20 mL was recorded by Kai Wang et al. (2020), when their group used 0.1 wt. % GO (Kai Wang 2020), while when GO was used by Rafieefar et al. (2021), it provided 9.2 mL of fluid loss at 0.15 wt. % (Rafieefar 2021). In the current work, the base mud loses 48 mL of filtrate

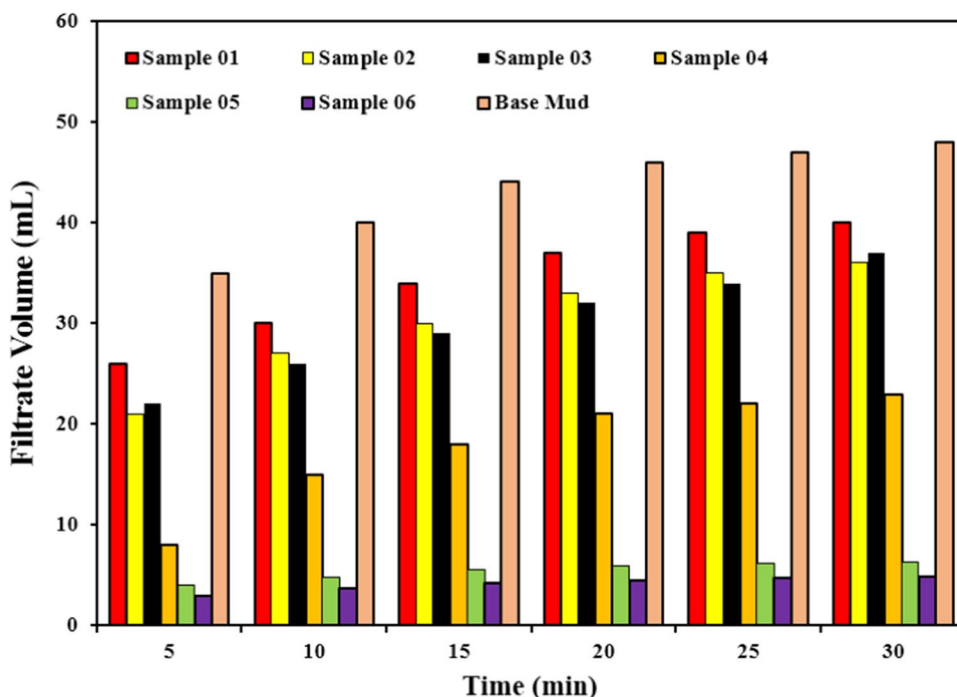
**Fig. 6** Gel strength of all the studied samples **a** GS 10 s, **b** GS 10 min



after 30 min of testing. This volume was substantial, and it shows that this type of WBM will not be feasible for drilling operations. However, as the NPs were added the filtrate loss started to get lower as shown in Fig. 7. The maximum fluid loss volume was 40 mL/30 min in Sample 1 (0.75 g of TiO<sub>2</sub> particle). On the other hand, minimum fluid loss volume was recorded in Sample 6 (2.25 g of GO/TiO<sub>2</sub> particle) 4.8 mL/30 min. This fluid loss volume was 7.5 times lower of what the TiO<sub>2</sub> particles provided at similar concentration. Additionally, it was below the filtrate volume loss recorded by different scholars, when used these

two particles as separate entities (Kai Wang 2020; Bayat and Shams 2019). The GO/TiO<sub>2</sub> sheet with its high surface area and high adsorption capacity adhere to the filter paper and block the micro and nanopore spaces. A superior barrier on the face of the filter paper is generated that prevents the penetration of water molecules. The GO assists TiO<sub>2</sub> in terms of more oxygen-bearing functional groups, which ultimately enhances the adsorptivity of GO/TiO<sub>2</sub> particles due to high ionic/electro communications, which reduces the fluid loss volume (Wang et al. 2019).

**Fig. 7** Effect of particle on filtrate volume loss



### Mud cake permeability, thickness and texture

One of the most critical properties of any drilling mud is to demonstrate minimum fluid loss volume. Wellbore instability, formation damage, and differential sticking are some of the most unwanted effects that arise with the filtrate loss from the mud. Therefore, an efficient mud system should demonstrate lower fluid loss volume along with the formation of fine, compacted mud cake and low permeability. According to the study conducted by Ikram et al. (2022), the mud cake thickness of commercial GO at 0.5 ppb was 1.13 mm (Ikram et al. 2022), which was lower than raw welding waste material and welding waste derived GO. Similarly, a study conducted on TiO<sub>2</sub> NPs by Bayat and Shams (2019). According to their study, TiO<sub>2</sub> NPs at 0.1 wt. % showed 0.17 cm and 1.00 mD of mud cake thickness and permeability of mud cake respectively (Bayat and Shams 2019). In the current work, the mud cake permeability and thickness of each sample in this study is shown in Fig. 8. The base mud with no concentration of NPs showed the maximum permeability of  $2.01 \times 10^{-4}$  mD. On the other hand, when NPs were added, sample 1 showed the maximum permeability of  $1.05 \times 10^{-4}$  mD. This sample contains the least concentration of TiO<sub>2</sub> particles. The mud cake thickness of 0.15 mm for this case was also higher than any other sample. However, as the concentration of TiO<sub>2</sub> particles increases in the mud system, permeability and thickness of the mud cake decreases. On the other hand, the mud sealing capacity improves considerably with the addition of GO/TiO<sub>2</sub> particles. When 2.25 g of GO/TiO<sub>2</sub> particles was added in

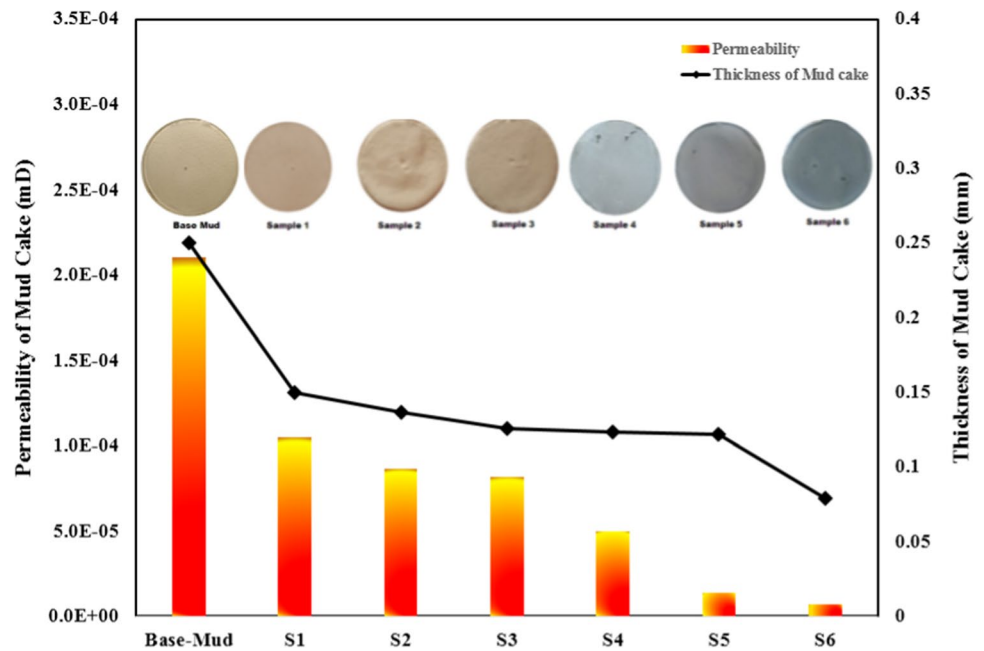
the base mud,  $w$  and  $t = 0.078$  mm was recorded. Almost 12 times reduction in permeability and  $2x$  time reduction in thickness was observed when compared with samples having exactly the same concentration of TiO<sub>2</sub>. Moreover, it was also performing better than the GO and TiO<sub>2</sub> results gather by Ikram et al. (2022) and Bayat and Shams (2019) respectively.

Figure 8 also displays the visuals of mud cake gathered after the filter press experiment. In the observation, it is apparent that as the quantity of the particle increases, the color of the mud cake becomes slightly dark. Moreover, the mud cake becomes dense, compacted and thin with an increase in the particle weight %. This clearly shows that the particles effectively block the permeation channels present on the filter paper and minimizes the water loss volume. The GO/TiO<sub>2</sub> particle increases the filtrate viscosity, thus reducing the filtration rate of the mud. The hydrogen bonding present between the functional groups in GO was the main cause of strong filter cake over the surface of filter paper. Furthermore, as the concentration of particles increases, the GO/TiO<sub>2</sub> particle creates a robust structure covering the micropores, and consequently, a decrease in fluid loss volume was recorded.

### Performance of KCl, PAC and GO/TiO<sub>2</sub> in shale swelling mitigation.

The performance of the synthesized GO/TiO<sub>2</sub> nanoparticles in terms of mitigating the shale swelling was compared with potassium chloride (KCl) and polyanionic cellulose (PAC).

**Fig. 8** Effect of particles on Mud cake permeability and thickness and texture



Full factorial design (FFD) of experiment methodology was implemented to study the efficacy of three additives in minimizing the shale swelling behavior. For the FFD, the concentration of particles in the WBM system was divided into two levels. Based on the mathematical expression of  $2^n = 8$  experimental runs were conducted. Figure 9a displays the importance of each particle in controlling the shale swelling through the Pareto chart. It can be observed that only GO/TiO<sub>2</sub> nanoparticles exceed the significance line, which clearly indicates the efficacy of this particle in controlling the penetration of water into the shale pellet. On the other hand, PAC and KCl were ineffective in mitigating the shale swelling characteristics. The interaction of these two entities was the main cause of their failure. The PAC is sensitive in presence of the monovalent and divalent cations (Mohamed Khodja et al. 2010). The presence of K<sup>+</sup> ions in the WBM system dehydrates the polymeric material leading to a decrease in fluid viscosity. Prior research has shown that low fluid viscosity high will be the filtration rate and lower shale swelling controlling behavior (Bülichen and Plank 2012). Therefore, the dehydration effect substantially reduces the performance of PAC.

The Pareto chart was further validated through an interaction plot as shown in Fig. 9b. All the three particles displayed a negative trend. This movement indicates that as the weight percentage of particles increases, there are some notable reductions in the shale swelling behavior. The increase in particle concentration will decrease shale swelling. The effect of both the particles on the shale swelling followed the following trend Shale swelling<sub>KCl</sub> > Shale swelling<sub>PAC</sub> > Shale swelling<sub>GO/TiO<sub>2</sub></sub>. Conversely, the quantity of the

particles follows a reverse order Concentration<sub>GO/TiO<sub>2</sub></sub> < Concentration<sub>PAC</sub> < Concentration<sub>KCl</sub>.

In addition, the interactive effects of the three particles with one another were also assessed using the 3D surface plots and contour plots as shown in Fig. 9c and d. The most effective interaction was observed between the nanoparticles and the polymeric material followed by nanoparticles with salt. The long chain of PAC interacted with GO/TiO<sub>2</sub> sheets to plug the pore spaces present in the shale pellet. Similar behavior was also observed in KCl and GO/TiO<sub>2</sub> sheets, which is also responsible for the minimization of fluid loss volume and maintaining the shale stability. However, the interaction between KCl and PAC was below par. As the concentration of both the particles increases in the mud system, a notable increase in fluid loss volume was recorded, which eventually decreases the shale stability. Sensitivity of PAC toward KCl was the main reason for their failure as a fluid loss control additive.

Figure 10 demonstrates the possible mechanism behind shale swelling mitigation through GO/TiO<sub>2</sub> particles. The shale surface becomes hydrophobic after its interaction with the GO/TiO<sub>2</sub> nanoparticle, thus preventing the penetration of water molecules into the shale nanoplatelets. In addition, the individual GO/TiO<sub>2</sub> sheets can plug the micropores and significantly reduce the water movement. Moreover, a GO/TiO<sub>2</sub> sheet has a strong tendency for creating an interparticle hydrogen bonding with its other sheets and other additives present in the system. Individual GO/TiO<sub>2</sub> plates could attract toward one another and prevent the migration of water from the mud into the shale structure.



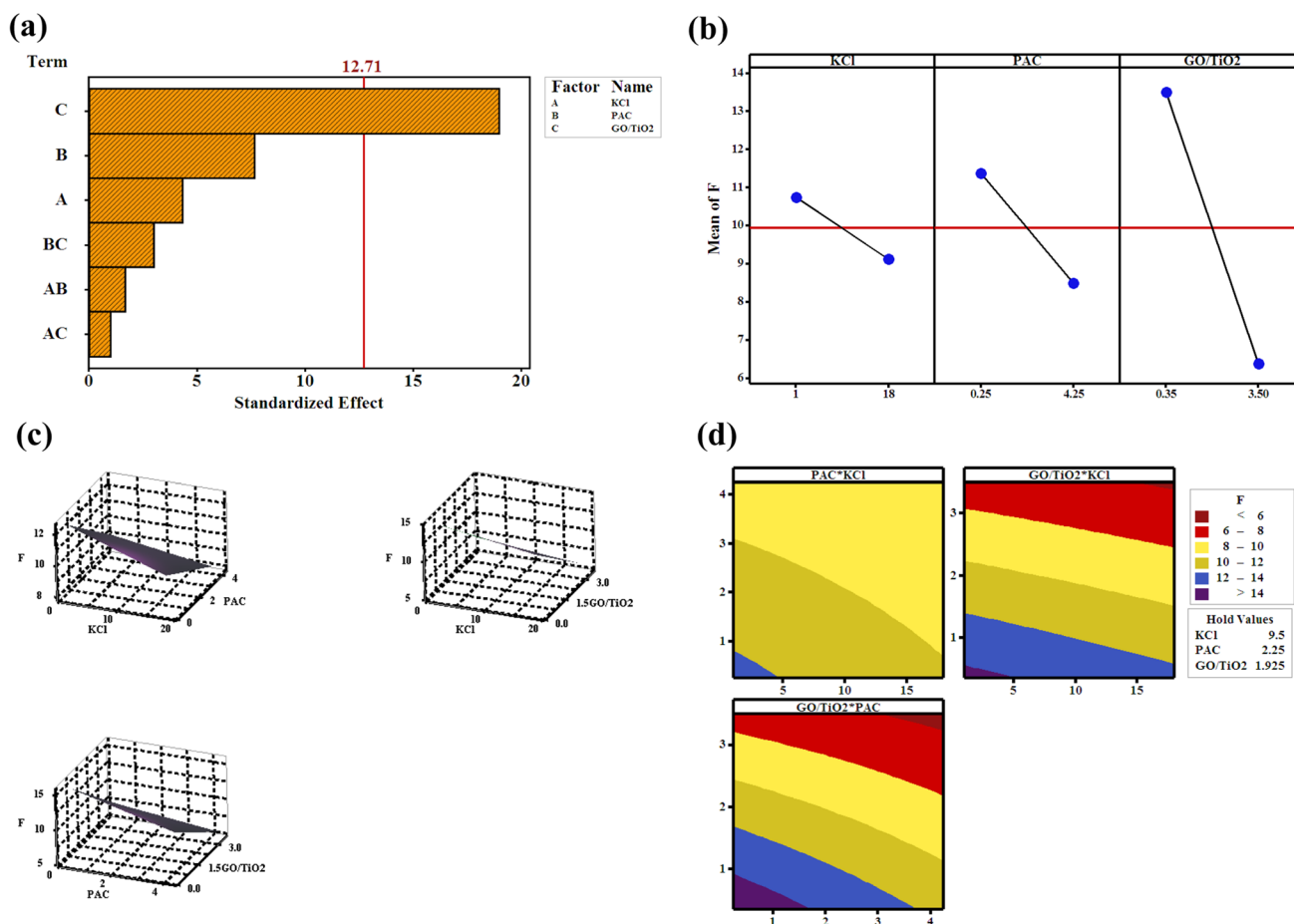


**Fig. 9** Factorial analysis on the shale swelling experiment **a** Pareto chart, **b** interaction plot, **c** 3D Surface plot, **d** contour plot

## Conclusion

The current study was divided into two parts. In the first part, GO/TiO<sub>2</sub> nanoparticles were synthesized using the hydrothermal method, which was then added in the WBM to improve its characteristics. The GO/TiO<sub>2</sub>-WBM properties were compared with anatase-TiO<sub>2</sub>-WBM. In the second part of the study, shale pellets were prepared in a hydraulic compactor, and interacted in LDSM with the WBM containing GO/TiO<sub>2</sub> nanoparticles, salt and polymer. The purpose was to investigate the influence of these entities on shale swelling behavior. The pertinent conclusions were drawn from the study:-

1. The presence of GO/TiO<sub>2</sub> nanoparticles greatly improved the rheological properties of WBM. The impact of GO/TiO<sub>2</sub> nanoparticles was far superior to the anatase-TiO<sub>2</sub>.
2. The GO supports TiO<sub>2</sub> through oxygen-bearing functional groups, which eventually improves the adsorptivity of GO/TiO<sub>2</sub> particles in the micro and nanopores

and reduces the filtrate loss volume. Almost 2.5 times reduction in fluid loss volume was noted in GO/TiO<sub>2</sub> particles.

3. The addition of GO/TiO<sub>2</sub> nanoparticles influences the mud cake's microstructure. Thin, compacted and lower permeability mud cake was obtained from GO/TiO<sub>2</sub>-WBM. The hydrogen bonding between the functional groups in GO was responsible for compactness of the filter cake
4. Based on the FFD design of the experiment, the GO/TiO<sub>2</sub> nanoparticles were the most influential particle in reducing the shale swelling and maintaining the well-bore integrity. These particles are responsible for developing a strong interparticle hydrogen bonding between its associated molecules, which prevents the fluid migration into shale pellets.
5. The impact of KCl and PAC on the shale swelling was relatively minor. The polymer PAC was dehydrated in presence of monovalent cations, which impacts their performance in minimizing the shale swelling.

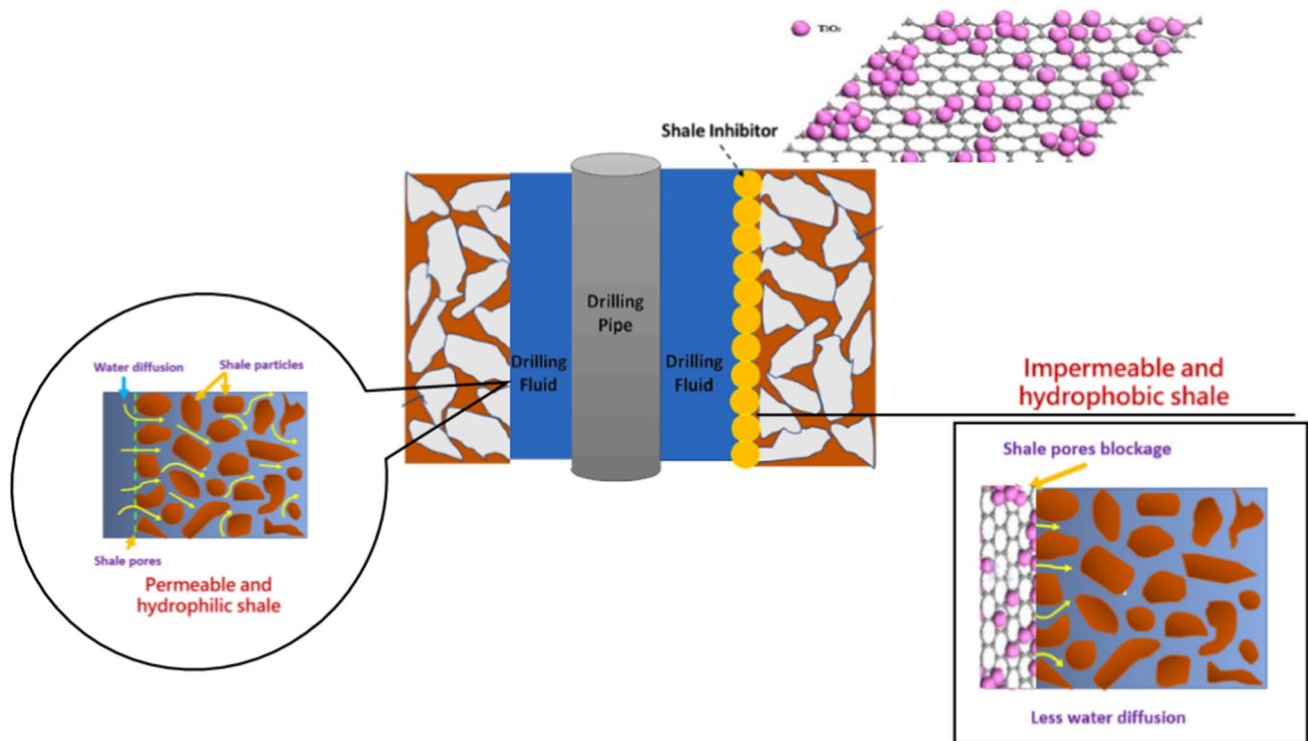


**Fig. 10** Schematic of shale swelling mitigation through GO/TiO<sub>2</sub> particle

Based on the findings, it can be decided that the performance of TiO<sub>2</sub> nanoparticles can substantially improve from graphene oxide support. Moreover, the GO/TiO<sub>2</sub> nanoparticles can act as a potential rheological modifier and fluid loss control agent in WBM systems, as its characteristics are superior to salt and polymeric materials.

**Funding** This is a self-funded project.

## Declarations

**Conflict of interest** The author declares that there is no conflict of interest between the co-authors.

## References

- Aftab AARI, Ismail AR, Khokhar S, Ibupoto ZH (2016) Novel zinc oxide nanoparticles deposited acrylamide composite used for enhancing the performance of water-based drilling fluids at elevated temperature conditions. *J Pet Sci Eng* 146:1142–1157
- Aftab A, Ismail AR, Ibupoto ZH, Akeiber H, Malghani MGK (2017) Nanoparticles based drilling muds a solution to drill elevated temperature wells: a review. *Renew Sustain Energy Rev* 76:1301–1313
- Aftab A, Ali M, Arif M, Panhwar S, Saady NMC, Al-Khdheawi EA, Iglauer S (2020) Influence of tailor-made TiO<sub>2</sub>/API bentonite nanocomposite on drilling mud performance: towards enhanced drilling operations. *Appl Clay Sci* 199:105862
- Ahmed N, Alam MS, Salam MA (2020) Experimental analysis of drilling fluid prepared by mixing iron (III) oxide nanoparticles with a KCl–Glycol–PHPA polymer-based mud used in drilling operation. *J Petrol Explor Prod Technol* 10:3389–3397
- Ali I, Ahmad M, Ganat TAA (2022) Experimental study on water-based mud: investigate rheological and filtration properties using cupressus cones powder. *J Pet Explor Prod Technol* 12(10):2699–2709
- Ali Ghayedi AK (2020) Laboratory investigation of the effect of GO–ZnO nanocomposite on drilling fluid properties and its potential on H<sub>2</sub>S removal in oil reservoirs. *J Petrol Sci Eng* 184:106684
- Alsaba M, Al Marshad A, Abbas A, Abdulkareem T, Al-Shammary A, Al-Ajmi M, Kebeish E (2020) Laboratory evaluation to assess the effectiveness of inhibitive nano-water-based drilling fluids for Zubair shale formation. *J Pet Explor Prod Technol* 10:419–428
- Altomare M, Dozzi MV, Chiarello GL, Di Paola A, Palmisano L, Selli E (2015) High activity of brookite TiO<sub>2</sub> nanoparticles in the photocatalytic abatement of ammonia in water. *Catal Today* 252:184–189
- Alvi MAA, Belayneh M, Bandyopadhyay S, Minde MW (2020) Effect of iron oxide nanoparticles on the properties of water-based drilling fluids. *Energies* 13(24):6718
- Aramendiz J, Imqam A (2020a) Silica and graphene oxide nanoparticle formulation to improve thermal stability and inhibition capabilities of water-based drilling fluid applied to woodford shale. *SPE Drill Completion* 35(02):164–179
- Bayat AE, Shams R (2019) Appraising the impacts of SiO<sub>2</sub>, ZnO and TiO<sub>2</sub> nanoparticles on rheological properties and shale inhibition of water-based drilling muds. *Coll Surf A Physicochem Eng Asp* 581:123792
- Bayat AE, Moghanloo PJ, Piroozian A, Rafati R (2018a) Experimental investigation of rheological and filtration properties of water-based drilling fluids in presence of various nanoparticles. *Coll Surf A Physicochem Eng Asp* 555:256–263

- Bayat AE, Harati S, Kolivandi H (2021) Evaluation of rheological and filtration properties of a polymeric water-based drilling mud in presence of nano additives at various temperatures. *Coll Surf A Physicochem Eng Asp* 627:127128
- Beg M, Kumar P, Choudhary P, Sharma S (2020) Effect of high temperature ageing on TiO<sub>2</sub> nanoparticles enhanced drilling fluids: a rheological and filtration study. *Upstream Oil Gas Technol* 5:100019
- Biwott TK (2019) Ambrose & Akaranta, Onyewuchi and Boniface, Oriji, *Terminalia mantaly leaves as a novel additive in water-based drilling MUD*. *Int J Chem Sci* 7:2173–2181
- P J Boul, B R Reddy, H Matt O'Connell, T Pete, C Thaemlitz (2016) Functionalized nanosilicas as shale inhibitors in water-based drilling fluids in Paper presented at the Offshore Technology Conference, SPE, Editor. Houston, Texas, USA
- Büllichen D, Plank J (2012) Role of colloidal polymer associates for the effectiveness of hydroxyethyl cellulose as a fluid loss control additive in oil well cement. *J Appl Polym Sci* 126(S1):E25–E34
- Chang W, Leong YK (2014) Ageing and collapse of bentonite gels—effects of Li, Na K and Cs Ions. *Rheol Acta* 53:109–122
- Dankwa OK, Appau PO, Broni-Bediako E (2018) Evaluating the effects of monovalent and divalent salts on the rheological properties of water based mud. *Open Pet Eng J* 11(1):98–106
- Elkatatny S (2019) Enhancing the rheological properties of water-based drilling fluid using micronized starch. *Arab J Sci Eng* 44:5433–5442
- K P Hoelscher, G De Stefano, M Riley, S Young (2012). Application of nanotechnology in drilling fluids. In: Paper presented at the SPE international oilfield nanotechnology conference and exhibition Noordwijk, The Netherlands
- Ikram R, Jan BM, Ahmad W, Sidek A, Khan M, Kenanakis G (2022) Rheological investigation of welding waste-derived graphene oxide in water-based drilling fluids. *Materials* 15(22):8266
- Institute (2017) A.P. Recommended practice for field testing water-based drilling fluids, in API RP 13B-1., API
- Jankovic A, Chaudhary G, Goia F (2021) Designing the design of experiments (DOE)—an investigation on the influence of different factorial designs on the characterization of complex systems. *Energ Build* 250:111298
- Khodja M, Canselier JP, Bergaya F, Fourar K, Khodja M, Cohaut N, Benmounah A (2010) Shale problems and water-based drilling fluid optimisation in the Hassi Messaoud Algerian oil field. *Appl Clay Sci* 49(4):383–393
- Kumar R, Kumar M, Kumar A, Singh R, Kashyap R, Rani S, Kumar D (2019) Surface modification of graphene oxide using esterification. *Mater Today Proc* 18:1556–1561
- Lalji SM, Ali SI, Ahmed R et al (2022) Influence of graphene oxide on salt-polymer mud rheology and Pakistan shale swelling inhibition behavior. *Arab J Geosci* 15:612
- Lalji SM, Ali SI, Asad M (2023) Experimental effect of biopolymers, synthetic and modified polymers on Western Pakistan shale (GHAZIJ) stability. *Arab J Sci Eng* 48:16639–16653
- Lalji SM, Ali SI, Ullah R et al (2023a) Experimental investigation of rheological behaviour and stability of mud system using novel image processing application in presence of activated carbon and silica-coated iron oxide nanoparticles. *Appl Nanosci* 13:6405–6420
- Lalji SM, Ali SI, Khan MA et al (2023b) Investigation of rheological behavior, filtration characteristics and microbial activity of biopolymer water-based drilling fluids containing monovalent and divalent cations. *Chem Pap* 77:4693–4704
- Lalji SM, Khan MA, Haneef J et al (2023c) Nano-particles adapted drilling fluids for the swelling inhibition for the Northern region clay formation of Pakistan. *Appl Nanosci* 13:503–517
- Lam C, Martin PJ, Jefferis SA (2015) Rheological properties of PHPA polymer support fluids. *J Mater Civ Eng* 27(11):04015021
- Liu X, Ma D, Tang H, Tan L, Xie Q, Zhang Y, Yao S (2014) Poly-amidoamine dendrimer and oleic acid-functionalized graphene as biocompatible and efficient gene delivery vectors. *ACS Appl Mater Interfaces* 6(11):8173–8183
- Ma J, Pang S, Zhang Z, Xia B, An Y (2021) Experimental study on the polymer/graphene oxide composite as a fluid loss agent for water-based drilling fluids. *ACS Omega* 6(14):9750–9763
- Minakov AV, Mikhienkova EI, Zhigarev VA et al (2018) A study of the influence of nanoparticles on the properties of drilling fluids. *Coll J* 80:418–426
- Nethravathi C, Rajamathi M (2008) Chemically modified graphene sheets produced by the solvothermal reduction of colloidal dispersions of graphite oxide. *Carbon* 46(14):1994–1998
- Nguyen-Phan TD, Pham VH, Shin EW, Pham HD, Kim S, Chung JS, Hur SH (2011) The role of graphene oxide content on the adsorption-enhanced photocatalysis of titanium dioxide/graphene oxide composites. *Chem Eng J* 170(1):226–232
- Parizad A, Ghahfarokhi AK, Shahbazi K, Daryasafar A, Sayahi T, Meybodi MK (2019) Experimental investigation of the effect of TiO<sub>2</sub> nanofluid and KCl salt on polymeric water-based drilling fluid properties. *Oil Gas Sci Technol Revue d'IFP Energ Nouvelles* 74:9
- Ponmani S, Nagarajan R, Sangwai JS (2016) Effect of nanofluids of CuO and ZnO in polyethylene glycol and polyvinylpyrrolidone on the thermal, electrical, and filtration-loss properties of water-based drilling fluids. *SPE J* 21:405–415
- Rafieefar A, Sharif F, Hashemi A, Bazargan AM (2021) Rheological behavior and filtration of water-based drilling fluids containing graphene oxide: experimental measurement, mechanistic understanding, and modeling. *ACS Omega* 6(44):29905–29920
- Reghunath S, Pinheiro D, Sunaja Devi KR (2021) A review of hierarchical nanostructures of TiO<sub>2</sub>: advances and applications. *Appl Surf Sci Adv* 3:100063
- Romanchuk AY, Slesarev AS, Kalmykov SN, Kosynkin DV, Tour JM (2013) Graphene oxide for effective radionuclide removal. *Phys Chem Chem Phys* 15(7):2321–2327
- Sharma M, Behl K, Nigam S, Joshi M (2018) TiO<sub>2</sub>-GO nanocomposite for photocatalysis and environmental applications: a green synthesis approach. *Vacuum* 156:434–439
- Shen J, Yan B, Shi M, Ma H, Li N, Ye M (2011) One step hydrothermal synthesis of TiO<sub>2</sub>-reduced graphene oxide sheets. *J Mater Chem* 21(10):3415–3421
- Sundar LS, Sharma KV, Naik MT, Singh MK (2013) Empirical and theoretical correlations on viscosity of nanofluids: a review. *Renew Sustain Energ Rev* 25:670–686
- Wajheuddin M, Hossain ME (2018) Development of an environmentally-friendly water-based mud system using natural materials. *Arab J Sci Eng* 43:2501–2513
- Wang R, Shi K, Huang D, Zhang J, An S (2019) Synthesis and degradation kinetics of TiO<sub>2</sub>/GO composites with highly efficient activity for adsorption and photocatalytic degradation of MB. *Sci Rep* 9(1):18744
- Wang K, Jiang G, Li X, Luckham PF (2020) Study of graphene oxide to stabilize shale in water-based drilling fluids. *Coll Surf A Physicochem Eng Asp* 606:125457
- You P, Yang Y, Wang M, Huang X, Huang X (2015) Graphene oxide-based nanocarriers for cancer imaging and drug delivery. *Curr Pharm Design* 21(22):3215–3222
- Yu J, Su Y, Cheng B, Zhou M (2006) Effects of pH on the microstructures and photocatalytic activity of mesoporous nanocrystalline titania powders prepared via hydrothermal method. *J Mole Catal A Chem* 258(1–2):104–112
- Yusaf T, Mahamude ASF, Farhana K, Harun WSW, Kadrigama K, Ramasamy D, Dhahad HA (2022) A comprehensive review on graphene nanoparticles: preparation, properties, and applications. *Sustainability* 14(19):12336

Z Deng, P W Livanec, J.P. Deville (2015). Novel Water-based fluids for oil-Sands drilling, in SPE Canada Heavy Oil Technical Conference, SPE, Editor: Calgary, Alberta, Canada

**Publisher's Note** Springer Nature remains neutral with regard to jurisdictional claims in published maps and institutional affiliations.

Springer Nature or its licensor (e.g. a society or other partner) holds exclusive rights to this article under a publishing agreement with the author(s) or other rightsholder(s); author self-archiving of the accepted manuscript version of this article is solely governed by the terms of such publishing agreement and applicable law.